

See discussions, stats, and author profiles for this publication at: <https://www.researchgate.net/publication/262530788>

Simultaneous Enhancement of Electron Injection and Air Stability in N-Type Organic Field-Effect Transistors by Water-Soluble Polyfluorene Interlayers

ARTICLE in ACS APPLIED MATERIALS & INTERFACES · MAY 2014

Impact Factor: 6.72 · DOI: 10.1021/am500466q · Source: PubMed

CITATIONS

3

READS

50

8 AUTHORS, INCLUDING:



Dongyoon Khim

Imperial College London

54 PUBLICATIONS 752 CITATIONS

SEE PROFILE



Rira Kang

Gwangju Institute of Science and Technology

9 PUBLICATIONS 74 CITATIONS

SEE PROFILE



Seung-Hoon Lee

Gwangju Institute of Science and Technology

16 PUBLICATIONS 97 CITATIONS

SEE PROFILE



Kang-Jun Baeg

Korea Electrotechnology Research Institute-...

87 PUBLICATIONS 1,906 CITATIONS

SEE PROFILE

Simultaneous Enhancement of Electron Injection and Air Stability in N-Type Organic Field-Effect Transistors by Water-Soluble Polyfluorene Interlayers

Jihong Kim,[‡] Dongyoon Khim,[‡] Rira Kang,[‡] Seung-Hoon Lee,[‡] Kang-Jun Baeg,[§] Minji Kang,[‡] Yong-Young Noh,[†] and Dong-Yu Kim^{*,‡}

[‡]Heeger Center for Advanced Materials, School of Materials Science and Engineering, Department of Nanobio Materials and Electronics, Gwangju Institute of Science and Technology (GIST), 261 Cheomdan-gwagiro, Buk-gu, Gwangju 500-712, Republic of Korea

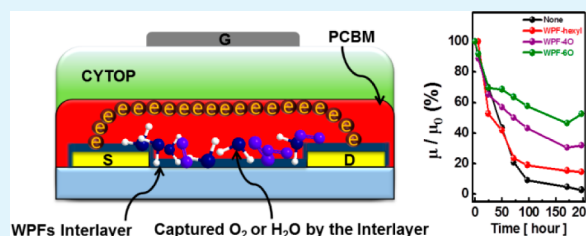
[§]Nano Carbon Materials Research Group, Korea Electrotechnology Research Institute (KERI), 12, Bulmosan-ro 10beon-gil, Seongsan-gu, Changwon, Gyeongsangnam-do 642-120, Republic of Korea

[†]Department of Energy and Materials Engineering, Dongguk University, 26 Pil-dong, 3 ga, Jung-gu, Seoul 100-715, Republic of Korea

Supporting Information

ABSTRACT: Here, we report the simultaneous attainment of efficient electron injection and enhanced stability under ambient conditions for top-gate/bottom-contact (TG/BC), n-type, organic field-effect transistors (OFETs) using water-soluble polyfluorene derivatives (WPFs). When inserting the WPF interlayers between a semiconductor and the BC Au electrodes, initially the ambipolar (6,6)-phenyl-C₆₁butyric acid methyl ester (PCBM) OFETs were fully converted to unipolar charge transport characteristics that were exclusively n-type with significantly increased electron mobilities as high as 0.12 cm²/(V s) and a decreased threshold voltage. These improvements were mostly attributed to the interfacial dipoles of WPF layers that aligned to form a favorable energy band structure for efficient electron injection and to effectively block counter charge carriers. These were confirmed when values for the reduced work function of metal electrodes with WPFs and their correlated contact resistance were measured via the ultraviolet photoemission spectroscopy and the transmission-line method, respectively. Moreover, the WPF interlayers played an important role in air stability of PCBM OFETs that exhibited higher and appreciably enhanced by increasing the ethylene-oxide side chain lengths of WPFs, which presumably was due to the water/oxygen/ion capturing effects in the hydrophilic interlayers.

KEYWORDS: organic field-effect transistors, conjugated polyelectrolytes, charge injection, interfacial dipoles, air-stability



INTRODUCTION

Over the past two decades, π -conjugated organic molecules have been extensively studied based on the complementary aspects of scientific interest and industrial benefit. These materials possess unique charge generation as well as transport and recombination properties that show promise for optoelectronics applications such as energy harvesting (organic photovoltaics (OPVs)),^{1–3} switching (organic field-effect transistors (OFETs)),^{4–6} and light-emitting devices (organic light-emitting diodes (OLEDs) and lasers).⁷ Moreover, these qualities enable the development of inexpensive soft electronics applications that result mostly from low-temperature and solution processability using a variety of cost-effective, large-area, high throughput graphic art printing techniques.^{8,9} In developing high-performance organic electronic devices, a number of approaches have been applied including the synthesis of new materials,^{10,11} post treatments for improving thin-film quality,¹² and interface engineering.^{13,14} The development of optimized materials that include active, electrode, and

dielectric layers is likely to be the best solution in order to realize high device performance.

However, it is quite difficult to simultaneously satisfy all requirements for commercial products such as OFETs with environmental/bias stability and organic semiconductors that have high charge carrier mobility, negligible interface traps, and small off-current, Ohmic contact to charge injection electrodes. Alternatively, interface engineering is one of the strategies that shows promise for the achievement of high-performance optoelectronic devices by extracting the maximum characteristics from a given material via surface treatment (e.g., oxygen plasma and self-assembled monolayers¹⁵) and the insertion of interlayers such as poly(3,4-ethylenedioxythiophene):poly(styrenesulfonate) (PEDOT:PSS),^{16,17} polyelectrolytes,^{18,19}

Received: January 22, 2014

Accepted: May 19, 2014

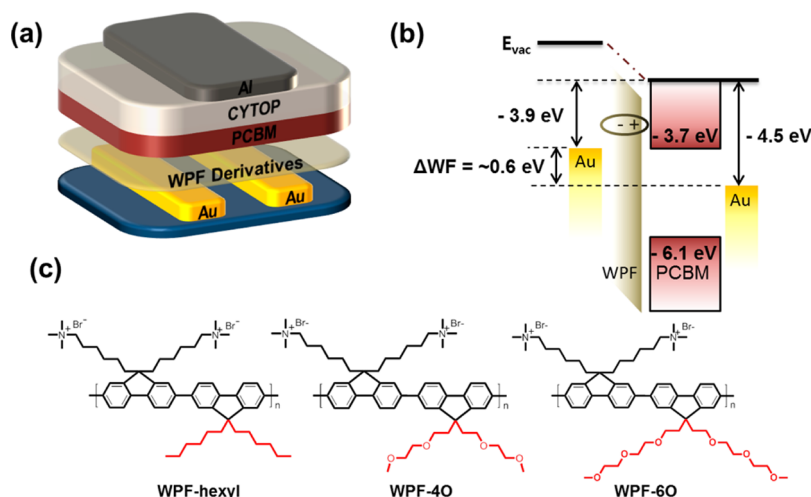


Figure 1. (a) Schematic diagram of a TG/BC OFET structure with WPF interlayers, (b) energy level diagram at the interface between semiconductor and Au S/D electrodes, and (c) the molecular structures of the WPF derivatives.

and inorganic compounds,^{20,21} between the contact electrodes and organic semiconductors.

Water-/alcohol-soluble conjugated polymers or conjugated polyelectrolytes (CPEs) have also been used in research as interlayers for various organic optoelectronic devices²² such as OLEDs,^{23,24} OPVs,^{25,26} and OFETs.²⁷ These interlayers have fulfilled critical roles in reducing the energy barriers for efficient charge injection/transport in many organic optoelectronic devices,²² which has been attributed mainly to an effectively tuned work function of metal electrodes that is induced either by permanent interfacial dipoles²⁸ or by ion migration²⁹ under the application of an electric field. Moreover, the high solubility of the CPEs in aqueous/alcoholic polar solvents easily allows the fabrication of multilayered devices via simple solution processing with no damage or intermixing with under-laid layers. Despite these many advantageous features of CPEs, a significant degradation in device performance has been noted after exposure to humid air because of the hydrophilic and hygroscopic nature of the CPEs. For this reason, there has been poorly understood and never been a report that documents how the structural feature and properties of a CPEs could affect the environmental stability of organic electronic devices over time under an ambient atmosphere.

As far as we could ascertain, this report is the first to document the simultaneous enhancement of device performance and air stability for n-type (6,6)-phenyl-C₆₁ butyric acid methyl ester (PCBM) OFETs through the introduction of the water-soluble polyfluorene derivatives (WPFs) as interlayers between semiconductor and bottom-contact (BC) source/drain electrodes. Initially, top-gated PCBM OFETs showed ambipolar charge transport characteristics with electron mobilities ($\mu_{FET,e}$) of ~ 0.045 cm²/(V s) and weak hole transport properties of $\mu_{FET,h} \approx 0.003$ cm²/(V s). On the other hand, the WPFs played an important role as an efficient electron-injection/hole-blocking layer, so that the PCBM OFETs fully converted to n-type only unipolar devices with a 3-fold increase in electron mobility of ~ 0.12 cm²/(V s). Moreover, we also noted that the PCBM OFETs with WPF interlayers showed an increased stability under ambient air conditions compared with devices with no interlayer. Interestingly, the air stability improved as the ethylene-oxide side chains of the WPFs increased, which could be mainly

attributed to the water/oxygen/ion capturing effects by hygroscopic/hydrophilic WPF moieties that prevented the trapping of mobile electrons at the semiconductor–dielectric interface.

EXPERIMENTAL METHODS

Field-Effect Transistor Fabrication. Corning Eagle XG glass was used as a substrate after sequential cleaning in an ultrasonic bath with deionized water, then acetone, then isopropanol. Source and drain electrodes of Au/Ni were patterned on substrates via conventional photolithography processing. WPF derivatives, WPF-hexyl, WPF-4O, and WPF-6O, were synthesized in our laboratory.⁴⁸ The WPF interlayers were dissolved in methanol and were deposited by spin-coating onto the Au-patterned substrates in a N₂-filled glovebox. The organic semiconductor material, PCBM was purchased from Nano-C and used as-received. The PCBM was dissolved in anhydrous chlorobenzene to make a 10 mg/mL solution that was then spin-coated. The semiconductor films were thermally annealed at 110 °C for 20 min to remove residual solvent under N₂ inert conditions. For a polymer dielectric layer, a CYTOP solution (Asahi Glass) was spin-coated onto the semiconductor layer. To remove the solvent, the films were baked for 2 h at 80 °C in the same N₂-filled glovebox. The Al gate electrode was deposited by thermal evaporation to achieve a film that was 50 nm thick with a shadow mask to complete fabrication of the TG/BC transistor.

Thin Film and Device Characterization. The thickness of the WPF layers and the surface morphology of the PCBM were investigated via tapping-mode AFM (Nanoscope III, Veeco Instruments, Inc.). The UPS measurement was carried out using an AXIS-NOVA (Kratos, Inc.) with a base pressure of 4.2×10^{-9} Torr. The current–voltage (*IV*) characteristics of the OFET devices were measured with a KEITHLEY 4200-SCS under nitrogen conditions at room temperature. The capacitance of the CYTOP was measured using an Agilent 4284A precision LCR meter and a KEITHLEY 4200-SCS at a frequency of 10 kHz. Air-stability was monitored by measuring the *IV* characteristics after keeping the OFET devices under an air atmosphere with humidity of 25%.

RESULTS AND DISCUSSION

Figure 1a shows a schematic diagram of the TG/BC OFET device structure. The staggered structure is a good configuration to use in discerning the charge injection effects through the interlayers on single metal electrodes because of the relatively low contact resistance (R_c) as a result of the large physical contact area and reduced current crowding effects

compared with the other coplanar device structures.³⁰ Moreover, hydroxyl-free polymer gate dielectrics³¹ in top-gated devices enable the study of nearly intrinsic ambipolar charge transport characteristics via excellent organic material compatibility and self-passivation effects³² compared with exposed active-layer, bottom-gate devices. To fabricate TG/BC OFETs based on solution-processed PCBM, we chose a CYTOP gate dielectric because the CYTOP will dissolve only in fluorinated orthogonal solvents that are perfect for the under-layer of most organic semiconductor layers including PCBM. Moreover, CYTOP has a low k , chemical stability, low surface energy, and hydrophobic dielectric properties, which allows it to provide excellent interfacial states that exhibit intrinsic charge transport properties even in commonly known unstable n-type semiconductors, such as PCBM.³³

As shown in Figure 2a, the transfer characteristics (the drain current (I_d) vs the gate voltage (V_g)) of the PCBM OFETs

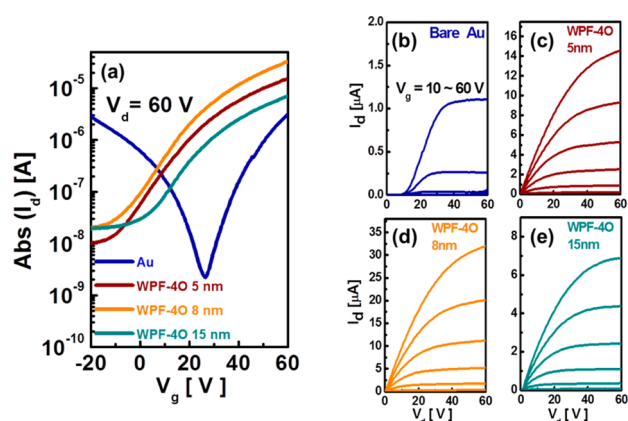


Figure 2. (a) Transfer characteristics of the n-channel in PCBM OFETs as the thickness of the WPF-4O interlayer increases. Output characteristics of the n-channel in PCBM OFETs (b) without a WPF-4O interlayer, and with interlayers of (c) 5, (d) 8, and (e) 15 nm ($W/L = 1.0$ mm/20 μ m).

using pristine Au electrodes showed clear ambipolar features with electron ($\mu_{\text{FET,e}}$) and hole mobilities ($\mu_{\text{FET,h}}$) of ~ 0.045 and ~ 0.003 $\text{cm}^2/(\text{V s})$, respectively, which were confirmed by typical V-shaped transfer curves in ambipolar transistors.³⁴ It was verified that our top-gated PCBM OFET devices can induce both electron (for n-type operation) and hole (for p-type operation) accumulations at the PCBM-CYTOP interface.³⁵ Notably, both electron and hole carriers could be injected from bare Au electrodes (measured metal work function $\Phi = -4.5$ eV) into the lowest unoccupied molecular orbital (LUMO = -3.7 eV) and the highest occupied molecular orbital (HOMO = -6.1 eV) levels, respectively, of a PCBM, and with appreciable electron and hole injection barrier heights of ~ 0.8 eV and ~ 1.6 eV, respectively (see Figure 1b). The

output curve (the I_d vs the drain voltage (V_d)) in Figure 2b also shows nonlinear behavior in the low V_d region, which is a clear evidence of the existence of a large R_c .

Figure 1c shows the molecular structures of the WPF interlayers with different ethylene oxide side chains: WPF-hexyl, -4O, and -6O. After inserting the WPFs between the BC Au source/drain (S/D) electrodes and the PCBM semiconductor layer, the initial ambipolar characteristics of the PCBM OFET devices were fully converted to an n-type only unipolar operation regime, as shown in Figure 2a. The $\mu_{\text{FET,e}}$ of the PCBM OFETs with a thickness-optimized (~ 8 nm) WPF-4O interlayer exhibited an approximate 3-fold increase (as high as 0.12 $\text{cm}^2/(\text{V s})$) and a reduced threshold voltage ($V_{\text{th,e}}$) of ~ 10.5 V. These developments were mostly attributed to the electron-injection and hole-blocking properties of the inserted WPF interlayers. Furthermore, it would also be attributed to the doping by ionic species which could act as a dopant.¹⁸ To determine the optimal thickness for an interlayer, we increased the WPF thickness by as much as 15 nm and found that the I_d and $\mu_{\text{FET,e}}$ in n-channel saturation region (at $V_d = 60$ V) were gradually enhanced at an interlayer thickness of ~ 8 nm. Beyond this critical thickness, however, the PCBM OFETs exhibited a degraded performance both in p-channel and n-channel operation regimes. The measured $\mu_{\text{FET,e}}$ of the PCBM OFETs with a 15 nm thick WPF-4O interlayer was decreased to 0.023 $\text{cm}^2/(\text{V s})$, which was an even lower value than that of a bare Au device with no interlayer. Fundamental device parameters such as $\mu_{\text{FET,e}}$, V_{th} , and the on/off-current ratios ($I_{\text{on}}/I_{\text{off}}$) of the PCBM OFETs with WPF-4O interlayer thicknesses that differed from 5 to 15 nm are summarized in Table 1.

Although there was a slight increase in the root-mean-square roughness (R_q) of from 0.24 to 0.40 nm with an increase in the interlayer film thickness of from 5 to 15 nm, respectively, we found no distinctive morphological changes in the atomic force microscopy (AFM) images of the surfaces of spin-coated PCBM active films either those with or without WPF-4O layers (see Figure 3). The π -conjugated organic molecules reportedly had a better-ordered morphology either on carbon-based electrodes³⁶ or on self-assembled monolayer-treated metal electrodes³⁷ than on the bare surface, which typically resulted in a reduced R_c and improved charge transport characteristics. Because of the similarities in the morphological features shown in the AFM images of the same semiconductor films—those with a bare Au and those with an interlayer—the dramatic enhancements of the performance of the n-type OFETs with a WPF interlayer could have been mostly the result of the modification of the interfacial energy states between the semiconductor and the BC electrodes.

Panels a and b in Figure 4 show the binding energy of electrons on an Au electrode surface from ultraviolet photoemission spectroscopy (UPS) and the measured value

Table 1. Device Parameters of the PCBM OFETs as the Thickness of WPF-4O is Increased^a

active layer	interlayer (thickness)	$\mu_{\text{FET,e}}$ ($\text{cm}^2/(\text{V s})$)	$I_{\text{on}}/I_{\text{off}}$	$V_{\text{th,e}}$ (V)	$R_c W$ ($\text{M}\Omega \text{ cm}$)	Φ (eV)
PCBM	none	$0.046 (\pm 0.01)$	$\sim 1 \times 10^4$	$29.3 (\pm 4.28)$	18.65	4.5
	WPF-4O (5 nm)	$0.084 (\pm 0.016)$	$\sim 1 \times 10^3$	$16.8 (\pm 4.85)$	0.12	3.9
	WPF-4O (8 nm)	$0.12 (\pm 0.03)$	$\sim 1 \times 10^3$	$10.5 (\pm 2.68)$	0.02	3.9
	WPF-4O (15 nm)	$0.023 (\pm 0.009)$	$\sim 1 \times 10^2$	$6.9 (\pm 2.71)$	0.09	3.8

^aThe electron field-effect mobilities ($\mu_{\text{FET,e}}$) were calculated in the saturation region ($V_d = 60$ V) using a standard device formula. CYTOP gate dielectric was ~ 500 nm thick ($C_i \approx 3.72$ nF cm^{-2}).

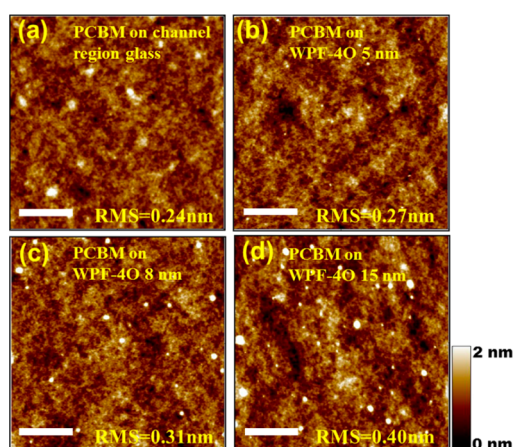


Figure 3. Height mode AFM images ($2 \mu\text{m} \times 2 \mu\text{m}$) of PCBM films (a) on a channel region without WPFs, (b) on a 5 nm thick WPF-4O layer, (c) on an 8 nm thick WPF-4O layer, (d) on a 15 nm thick WPF-4O layer. The scale bars are 500 nm.

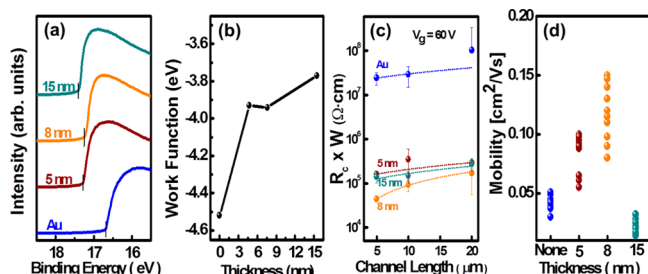


Figure 4. (a) UPS spectra, and (b) corresponding work functions of bare Au electrodes and those of WPF-4O layers with a different thickness on Au. (c) Channel width normalized contact resistance ($R_c W$) for electron injection, and (d) the distribution map of electron mobility ($\mu_{\text{FET},e}$) in PCBM OFETs based on bare Au electrodes and those of WPF-4O layers with a different thickness on Au.

of the work function (Φ) of metal electrodes as the thickness of WPF interlayers changes. The Φ of an Au electrode was remarkably reduced from -4.5 to -3.8 eV, as the WPF-4O layer thickness was increased from 0 to 15 nm. Notably, the thickness-optimized (~ 8 nm thick) WPF-4O layer induced the Φ of an Au electrode to a level of -3.9 eV, which matched well with the value of the LUMO level of a PCBM, at about -3.7 eV.³⁸ The R_c of PCBM OFETs for electron injection were evaluated using the transmission-line method (TLM) at $V_g = 60$ V. As shown in Figure 4c, the R_c of PCBM OFETs with a bare Au electrode was ~ 18.65 M Ω cm, but it was significantly reduced by approximately 3 orders of magnitude to 20 k Ω cm after the insertion of a WPF interlayer. The decreased R_c of WPFs-incorporated PCBM OFETs was attributed to a diminished electron injection barrier height between the LUMO level of PCBM and the Φ of Au electrodes (see schematic energy level diagram in Figure 1b). The improved electron injection efficiency was also confirmed in n-channel output characteristics, which showed output curves that were almost linear in the low V_d region, as shown in Figure 2c–e. In addition, the negative shift of V_{th} can be also explained by reducing R_c ^{39,40} because of the WPF-4O interlayer, which can substantially affect to the charge density or accumulation in the semiconductor. This indicates a clear reduction in the R_c by incorporating the WPFs as an electron injection layer. Therefore, the WPF interlayers make the top-gated PCBM

OFETs an n-type only unipolar device with high electron mobility and negligible p-type behaviors (see Figure 4d).

Note that π -conjugated polyelectrolyte (CPE) layers have typically played an important role in modifying the Φ of metal electrodes via ion migration and/or aligned permanent interfacial dipoles on the surface, thereby engineering the charge carrier injection/extraction properties in various optoelectronic devices.^{22,28,29} The interfacial dipoles in WPF interlayers are mostly induced between the two amine ionic salts or the ethylene oxide side chains,²⁵ where the dipole moment lies at the 9-position of WPF-4O and WPF-6O molecules.^{23,41} Most devices with a thin CPE layer (below 10 nm thick) could be affected by the interfacial dipoles,⁴² which agreed with our OFET results. Thin WPF-4O layers (5–8 nm thick) formed interfacial dipoles at the interface between the BC Au electrodes and the PCBM n-type semiconductor, which shifted up the vacuum level of Au electrodes and provided a favorable dipolar direction that enhanced the electron injection (see Figure 1b). Although very similar linear output characteristics persisted in the low V_d regions device performance of the OFETs with a thicker WPF-4O interlayer (about 15 nm thick) exhibited a relatively low $\mu_{\text{FET},e}$ of ~ 0.02 cm²/(V s), which was even below that of bare Au OFET devices. This could be explained by the interrupted charge carrier injection into a semiconductor active channel with a thickness that was beyond the critical interlayer amount (above ~ 8 nm), at which point the bulk insulating properties of the material started to dominate.^{15,43} In cases of overly thick WPF-4O interlayers (40–50 nm thick), the transistors were not operational.

Various WPFs with different ethylene oxide side chains from WPF-hexyl, -4O, and -6O (as shown in Figure 1c) were adopted as interlayers of the same OFETs in order to investigate how the different length would affect device performance. In our previous study, longer ethylene oxide side chains generally improved the power conversion efficiency in OPV devices due to an increase open circuit voltages by a reduction in the Φ of metallic cathodes.²⁵ The optimal thickness for a WPF-4O interlayer (8 nm thick) was also applied to the other interlayers: WPF-hexyl and WPF-6O. The PCBM OFETs showed similar device performances regardless of the side chains, as noted by the transfer characteristics shown in Figure 5a. The $\mu_{\text{FET},e}$ of PCBM OFETs with all types of WPF interlayers were improved to ~ 0.10 cm²/(V s), whereas the $V_{th,e}$ of the corresponding devices was gradually decreased from 10.8 to 5.8 V as ethylene oxide side chain length was increased (see Table 2). All WPF interlayers tuned the Φ of an Au

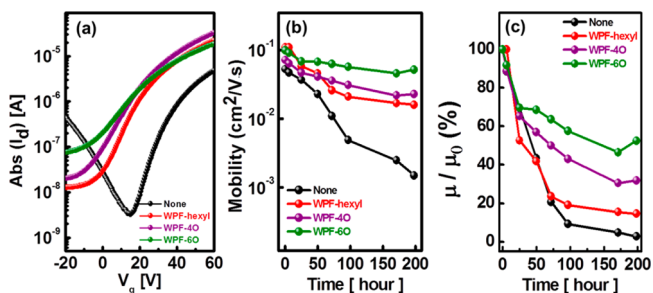
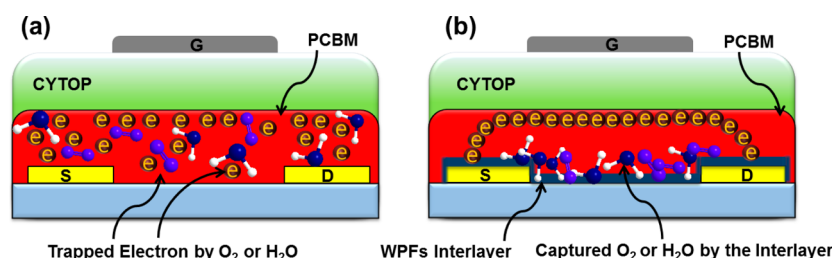


Figure 5. (a) Transfer characteristics (at $V_d = 60$ V) of the n-channel in PCBM OFETs without and with WPF injection layers. Evolution of (b) the electron field-effect mobility and (c) its normalized value as a function of time for PCBM OFETs exposed to ambient air with $\sim 25\%$ humidity.

Table 2. Device Parameters of the PCBM OFETs without and with Various WPF Interlayers^a

active layer	interlayer (thickness)	$\mu_{\text{FET},e}$ ($\text{cm}^2/(\text{V s})$)	$I_{\text{on}}/I_{\text{off}}$	$V_{\text{th},e}$ (V)	Φ (eV)
PCBM	None	0.046 (± 0.01)	$\sim 1 \times 10^4$	29.3 (± 4.28)	4.3
	WPF-hexyl (8 nm)	0.098 (± 0.025)	$\sim 1 \times 10^3$	10.8 (± 0.96)	3.6
	WPF-4O (8 nm)	0.12 (± 0.03)	$\sim 1 \times 10^3$	10.5 (± 2.68)	3.6
	WPF-6O (8 nm)	0.11 (± 0.029)	1×10^2 to 1×10^3	5.8 (± 1.47)	3.6

^aThe electron field-effect mobilities ($\mu_{\text{FET},e}$) were calculated in the saturation region (at $V_d = 60$ V) using a standard device formula. The CYTOP gate dielectric was ~ 500 nm in thickness (dielectric capacitance $C_i \approx 3.72$ nF/cm²).

**Figure 6.** Schematic illustration of the air stability of TG/BC PCBM OFETs, (a) without and (b) with a WPF interlayer.

electrode to the same value that was confirmed by UPS measurement (see Figure S1 in the Supporting Information), so the negligible electron injection barrier heights for BC Au electrodes via all WPF interlayers with different side chains had already contributed to the similar amounts of enhancements in n-type OFET characteristics.

Stability under ambient air conditions for n-type OFETs is also a very important issue for practical optoelectronics applications. Our PCBM OFETs with a WPF interlayer were exposed to ambient air with $\sim 25\%$ humidity, and device characteristics were monitored for about 200 h. In comparison with p-type organic semiconductors, the OFET properties of the n-type materials were more easily affected by O₂ and H₂O and degraded fast by trapped mobile electrons in an active channel.^{44,45} Figures 5b and 5c show the evolution of $\mu_{\text{FET},e}$ degradation in PCBM OFETs after exposure to air. For devices without the WPF interlayer, the $\mu_{\text{FET},e}$ was rapidly degraded and finally reached $\sim 1 \times 10^{-3}$ cm²/(V s) after 200 h exposure to air. It is noteworthy, that inserting the WPF interlayers significantly improved the air stability. In particular, the $\mu_{\text{FET},e}$ of a PCBM OFET using a WPF-6O layer was relatively stable and maintained about 0.05 cm²/(V s) even after 200 h in air. Notably, by changing the ethylene oxide side chains from WPF-hexyl to -4O and -6O, the overall performance of the n-type OFETs exhibited less degradation. The $\mu_{\text{FET},e}$ was stably maintained at higher values (exceeding 1×10^{-2} cm²/(V s)) after exposure to air for 200 h. For a quantitative comparison of the device stability, the normalized by initial value of $\mu_{\text{FET},e}$ are shown in Figure 5c. Without a WPF interlayer, the $\mu_{\text{FET},e}$ of the PCBM OFETs was rapidly decreased to about 2% of the initial value after 200 h, whereas it remained at $\sim 50\%$ for the OFETs with a WPF-6O interlayer. The other devices with WPF-hexyl and WPF-4O interlayers also showed better air stabilities as ~ 15 and $\sim 35\%$, respectively, of their initial values after 200 h. To the best of our knowledge, this is the first report of an improvement in the air stability of n-type OFETs by using a CPE electron-injection interlayer in the TG/BC device structure.

Although further study is needed to completely clarify the origin, there could be two possible origins of increasing air stability. First of all, we believe that the ammonium salt contained in the WPF interlayers could play a role of dopant.

It can be identified by a clear evidence of n-doping that shows the increased off-current from the transfer curves.¹⁸ It has been reported that doping in n-channel OFETs by n-type dopants enhanced the device air-stability^{46–48} and tetrabutyl ammonium salts induced efficient electron transfer to PCBM.⁴⁹ Therefore, it could be applied in our system that PCBM could be doped slightly by the ammonium salts in the WPF interlayers possibly increasing air-stability. However, it cannot be explained only by the doping of PCBM, which exhibited the better device air stability as increasing ethylene oxide side chain of the interlayers. Accordingly, we also believe that the hydrophilic and hygroscopic properties of the WPF molecules could effectively attract the polar oxygen and moisture molecules. Moreover, these interlayers may play the important role of a scavenger for the electron-trapping molecules (O₂ and H₂O) by preventing the diffusion of those molecules into the active channel region at the semiconductor–dielectric interface over time in air, as in Figure 6. Those capabilities improve when the hygroscopic interlayers have stronger oxygen- and moisture-attracting groups in the CPE molecules. In our previous report,⁵⁰ we also investigated the side-chain effect on the performance of various optoelectronic devices, which proved that hydrophilic properties increase as the ethylene-oxide side chains increase.

CONCLUSIONS

In conclusion, we studied the effect of various WPFs used as charge-injection interlayers between n-type organic semiconductor and Au BC electrodes. Obviously, it was successfully verified that the PCBM OFET characteristics were remarkably improved by incorporating the WPF layers, which significantly enhanced the n-channel characteristics with a $\mu_{\text{FET},e}$ that was increased to as high as 0.12 cm²/(V s), a reduced $V_{\text{th},e}$ and a smaller R_c for electron injection, whereas the p-channel properties were suppressed. Very thin (~ 8 nm thick) WPF interlayers introduced interfacial dipoles on the metal electrode surface so that a reduced Φ enabled a negligible electron injection energy barrier height at the metal–semiconductor interface. It is worth noting that the WPF interlayers resulted in excellent air stability even in relatively air-unstable n-type semiconductors, such as PCBM, and also that increasing the ethylene oxide side chains of the interlayers exhibited better

device stability due to both doping via ammonium salt and a stronger capability for capturing the oxygen and moisture molecules. On the basis of these results, our WPF interlayers could be very attractive from the aspects of an efficient electron-injection/hole-blocking layer and a bottom-laid passivation layer for a variety of optoelectronics applications.

■ ASSOCIATED CONTENT

● Supporting Information

UPS spectra of the various WPF derivatives interlayers with about 8 nm thickness on Au electrode surface, transfer characteristics as time goes by for 200 h without/with the interlayers, and contact angle of the WPF interlayers. This material is available free of charge via the Internet at <http://pubs.acs.org/>

■ AUTHOR INFORMATION

Corresponding Author

*E-mail: kimdy@gist.ac.kr.

Notes

The authors declare no competing financial interest.

■ ACKNOWLEDGMENTS

This work was supported by a National Research Foundation of Korea (NRF) grant funded by the Korea government (MSIP) (2013-059210, 2008-0062606, CELA-NCRC, and NRF-2009-C1AAA001-2009-0092950). Thanks are extended to the Heeger Center for Advanced Materials (HCAM) and to the Korea Basic Science Institute (KBSI) for the AFM and UPS measurements.

■ REFERENCES

- (1) Yu, G.; Gao, J.; Hummelen, J. C.; Wudl, F.; Heeger, A. J. Polymer Photovoltaic Cells: Enhanced Efficiencies via a Network of Internal Donor-Acceptor Heterojunctions. *Science* **1995**, *270*, 1789–1791.
- (2) Gunes, S.; Neugebauer, H.; Sariciftci, N. S. Conjugated Polymer-Based Organic Solar Cells. *Chem. Rev.* **2007**, *107*, 1324–1338.
- (3) Li, G.; Zhu, R.; Yang, Y. Polymer Solar Cells. *Nat. Photon* **2012**, *6*, 153–161.
- (4) Sirringhaus, H. Device Physics of Solution-Processed Organic Field-Effect Transistors. *Adv. Mater.* **2005**, *17*, 2411–2425.
- (5) Horowitz, G. Organic Field-Effect Transistors. *Adv. Mater.* **1998**, *10*, 365–377.
- (6) Di, C. A.; Zhang, F.; Zhu, D. Multi-Functional Integration of Organic Field-Effect Transistors (OFETs): Advances and Perspectives. *Adv. Mater.* **2013**, *25*, 313–330.
- (7) Burroughes, J. H.; Bradley, D. D. C.; Brown, A. R.; Marks, R. N.; Mackay, K.; Friend, R. H.; Burns, P. L.; Holmes, A. B. Light-Emitting Diodes Based on Conjugated Polymers. *Nature* **1990**, *347*, 539–541.
- (8) Facchetti, A. π -Conjugated Polymers for Organic Electronics and Photovoltaic Cell Applications. *Chem. Mater.* **2011**, *23*, 733–758.
- (9) Moonen, P. F.; Yakimets, I.; Huskens, J. Fabrication of Transistors on Flexible Substrates: from Mass-Printing to High-Resolution Alternative Lithography Strategies. *Adv. Mater.* **2012**, *24*, 5526–5541.
- (10) Yan, H.; Chen, Z.; Zheng, Y.; Newman, C.; Quinn, J. R.; Dotz, F.; Kastler, M.; Facchetti, A. A High-Mobility Electron-Transporting Polymer for Printed Transistors. *Nature* **2009**, *457*, 679–687.
- (11) He, Z.; Zhong, C.; Su, S.; Xu, M.; Wu, H.; Cao, Y. Enhanced Power-Conversion Efficiency in Polymer Solar Cells Using an Inverted Device Structure. *Nat. Photon* **2012**, *6*, 591–595.
- (12) Khim, D.; Baeg, K.-J.; Kim, J.; Kang, M.; Lee, S.-H.; Chen, Z.; Facchetti, A.; Kim, D.-Y.; Noh, Y.-Y. High Performance and Stable N-Channel Organic Field-Effect Transistors by Patterned Solvent-Vapor Annealing. *ACS Appl. Mater. Interfaces* **2013**, *5*, 10745–10752.
- (13) Baeg, K.-J.; Kim, J.; Khim, D.; Jung, S.-W.; Kang, M.; You, I.-K.; Kim, D.-Y.; Facchetti, A.; Noh, Y.-Y. Remarkable Enhancement of Hole Transport in Top-Gated N-Type Polymer Field-Effect Transistors by a High-k Dielectric for Ambipolar Electronic Circuits. *Adv. Mater.* **2012**, *24*, 5433–5439.
- (14) Acton, O.; Dubey, M.; Weidner, T.; O'Malley, K. M.; Kim, T.-W.; Ting, G. G.; Hutchins, D.; Baio, J. E.; Lovejoy, T. C.; Gage, A. H.; Castner, D. G.; Ma, H.; Jen, A. K.-Y. Simultaneous Modification of Bottom-Contact Electrode and Dielectric Surfaces for Organic Thin-Film Transistors Through Single-Component Spin-Cast Monolayers. *Adv. Funct. Mater.* **2011**, *21*, 1476–1488.
- (15) Gooding, J. J.; Ciampi, S. The Molecular Level Modification of Surfaces: from Self-Assembled Monolayers to Complex Molecular Assemblies. *Chem. Soc. Rev.* **2011**, *40*, 2704–2718.
- (16) Brown, T. M.; Kim, J. S.; Friend, R. H.; Cacialli, F.; Daik, R.; Feast, W. J. Built-in Field Electroabsorption Spectroscopy of Polymer Light-Emitting Diodes Incorporating a Doped Poly(3,4-ethylene dioxathiophene) Hole Injection Layer. *Appl. Phys. Lett.* **1999**, *75*, 1679–1681.
- (17) Yeo, J.-S.; Yun, J.-M.; Kim, D.-Y.; Park, S.; Kim, S.-S.; Yoon, M.-H.; Kim, T.-W.; Na, S.-I. Significant Vertical Phase Separation in Solvent-Vapor-Annealed Poly(3,4-ethylenedioxythiophene):Poly(styrene sulfonate) Composite Films Leading to Better Conductivity and Work Function for High-Performance Indium Tin Oxide-Free Optoelectronics. *ACS Appl. Mater. Interfaces* **2012**, *4*, 2551–2560.
- (18) Zhou, Y.; Fuentes-Hernandez, C.; Shim, J.; Meyer, J.; Giordano, A. J.; Li, H.; Winget, P.; Papadopoulos, T.; Cheun, H.; Kim, J.; Fenoll, M.; Dindar, A.; Haske, W.; Najafabadi, E.; Khan, T. M.; Sojoudi, H.; Barlow, S.; Graham, S.; Brédas, J.-L.; Marder, S. R.; Kahn, A.; Kippelen, B. A Universal Method to Produce Low Work Function Electrodes for Organic Electronics. *Science* **2012**, *336*, 327–332.
- (19) He, Z. C.; Zhong, C.; Huang, X.; Wong, W.-Y.; Wu, H.; Chen, L.; Su, S.; Cao, Y. Simultaneous Enhancement of Open-Circuit Voltage, Short-Circuit Current Density, and Fill Factor in Polymer Solar Cells. *Adv. Mater.* **2011**, *23*, 4636–4643.
- (20) Baeg, K.-J.; Kim, J.; Khim, D.; Caironi, M.; Kim, D.-Y.; You, I.-K.; Quinn, J. R.; Facchetti, A.; Noh, Y.-Y. Charge Injection Engineering of Ambipolar Field-Effect Transistors for High-Performance Organic Complementary Circuits. *ACS Appl. Mater. Interfaces* **2011**, *3*, 3205–3214.
- (21) Minari, T.; Darmawan, P.; Liu, C.; Li, Y.; Xu, Y.; Tsukagoshi, K. Highly Enhanced Charge Injection in Thienoacene-Based Organic Field-Effect Transistors with Chemically Doped Contact. *Appl. Phys. Lett.* **2012**, *100*, 093303.
- (22) Hoven, C. V.; Garcia, A.; Bazan, G. C.; Nguyen, T. Q. Recent Applications of Conjugated Polyelectrolytes in Optoelectronic Devices. *Adv. Mater.* **2008**, *20*, 3793–3810.
- (23) Oh, S.-H.; Vak, D.; Na, S.-I.; Lee, T.-W.; Kim, D.-Y. Water-Soluble Polyfluorenes as an Electron Injecting Layer in PLEDs for Extremely High Quantum Efficiency. *Adv. Mater.* **2008**, *20*, 1624–1629.
- (24) Zhong, C.; Liu, S.; Huang, F.; Wu, H.; Cao, Y. Highly Efficient Electron Injection from Indium Tin Oxide/Cross-Linkable Amino-Functionalized Polyfluorene Interface in Inverted Organic Light Emitting Devices. *Chem. Mater.* **2011**, *23*, 4870–4876.
- (25) Oh, S.-H.; Na, S.-I.; Jo, J.; Lim, B.; Vak, D.; Kim, D.-Y. Water-Soluble Polyfluorenes as an Interfacial Layer Leading to Cathode-Independent High Performance of Organic Solar Cells. *Adv. Funct. Mater.* **2010**, *20*, 1977–1983.
- (26) Seo, J. H.; Gutacker, A.; Sun, Y.; Wu, H.; Huang, F.; Cao, Y.; Scherf, U.; Heeger, A. J.; Bazan, G. C. Improved High-Efficiency Organic Solar Cells via Incorporation of a Conjugated Polyelectrolyte Interlayer. *J. Am. Chem. Soc.* **2011**, *133*, 8416–8419.
- (27) Seo, J. H.; Gutacker, A.; Walker, B.; Cho, S.; Garcia, A.; Yang, R.; Nguyen, T.-Q.; Heeger, A. J.; Bazan, G. C. Improved Injection in n-Type Organic Transistors with Conjugated Polyelectrolytes. *J. Am. Chem. Soc.* **2009**, *131*, 18220–18221.

- (28) Crispin, X.; Geskin, V.; Crispin, A.; Cornil, J.; Lazzaroni, R.; Salaneck, W. R.; Bredas, J. L. Characterization of the Interface Dipole at Organic/Metal Interfaces. *J. Am. Chem. Soc.* **2002**, *124*, 8131–8141.
- (29) Hoven, C.; Yang, R.; Garcia, A.; Heeger, A. J.; Nguyen, T. Q.; Bazan, G. C. Ion Motion in Conjugated Polyelectrolyte Electron Transporting Layers. *J. Am. Chem. Soc.* **2007**, *129*, 10976–10977.
- (30) Richards, T. J.; Sirringhaus, H. Analysis of the Contact Resistance in Staggered, Top-Gate Organic Field-Effect Transistors. *J. Appl. Phys.* **2007**, *102*, 094510.
- (31) Yoon, M.-H.; Kim, C.; Facchetti, A.; Marks, T. J. Gate Dielectric Chemical Structure–Organic Field-Effect Transistor Performance Correlations for Electron, Hole, and Ambipolar Organic Semiconductors. *J. Am. Chem. Soc.* **2006**, *128*, 12851–12869.
- (32) Sirringhaus, H.; Kawase, T.; Friend, R. H. High-Resolution Inkjet Printing of All-Polymer Transistor Circuits. *Science* **2000**, *290*, 2123–2126.
- (33) Veres, J.; Ogier, S. D.; Leeming, S. W.; Cupertino, D. C.; Khaffaf, S. M. Low- k Insulators as the Choice of Dielectrics in Organic Field-Effect Transistors. *Adv. Funct. Mater.* **2003**, *13*, 199–204.
- (34) Anthopoulos, T. D.; de Leeuw, D. M.; Cantatore, E.; Setayesh, S.; Meijer, E. J.; Tanase, C.; Hummelen, J. C.; Blom, P. W. M. Organic Complementary-Like Inverters Employing Methanofullerene-Based Ambipolar Field-Effect Transistors. *Appl. Phys. Lett.* **2004**, *85*, 4205–4207.
- (35) Wobkenberg, P. H.; Eda, G.; Leem, D.-S.; De Mello, J. C.; Bradley, D. D. C.; Chhowalla, M.; Anthopoulos, T. D. Reduced Graphene Oxide Electrodes for Large Area Organic Electronics. *Adv. Mater.* **2011**, *23*, 1558–1562.
- (36) Becerril, H. A.; Stoltenberg, R. M.; Tang, M. L.; Roberts, M. E.; Liu, Z.; Chen, Y.; Kim, D. H.; Lee, B. L.; Lee, S.; Bao, Z. Fabrication and Evaluation of Solution-Processed Reduced Graphene Oxide Electrodes for p- and n-Channel Bottom-Contact Organic Thin-Film Transistors. *ACS Nano* **2010**, *4*, 6343–6352.
- (37) Park, S. K.; Mounney, D. A.; Subramanian, S.; Anthony, J. E.; Jackson, T. N. High-Mobility Spin-Cast Organic Thin Film Transistors. *Appl. Phys. Lett.* **2008**, *93*, 043301.
- (38) Anthopoulos, T. D.; Tanase, C.; Setayesh, S.; Meijer, E. J.; Hummelen, J. C.; Blom, P. W. M.; de Leeuw, D. M. Ambipolar Organic Field-Effect Transistors Based on a Solution-Processed Methanofullerene. *Adv. Mater.* **2004**, *16*, 2174–2179.
- (39) Yan, X.; Wang, J.; Wang, H.; Wang, H.; Yan, D. Improved n-type Organic Transistors by Introducing Organic Heterojunction Buffer Layer under Source/Drain Electrodes. *Appl. Phys. Lett.* **2006**, *89*, 053510.
- (40) Khim, D.; Baeg, K.-J.; Kim, J.; Yeo, J.-S.; Kang, M.; Amegadzea, P. S. K.; Kim, M.-G.; Cho, J.; Lee, J. H.; Kim, D.-Y.; Noh, Y.-Y. Electron Injection Enhancement by a Cs-Salt Interlayer in Ambipolar Organic Field-Effect Transistors and Complementary Circuits. *J. Mater. Chem.* **2012**, *22*, 16979–16985.
- (41) Oh, S.-H.; Na, S.-I.; Nah, Y.-C.; Vak, D.; Kim, S.-S.; Kim, D.-Y. Novel Cationic Water-Soluble Polyfluorene Derivatives with Ion-Transporting Side Groups for Efficient Electron Injection in PLEDs. *Org. Electron.* **2007**, *8*, 773–783.
- (42) Lin, C. Y.; Garcia, A.; Zalar, P.; Brzezinski, J. Z.; Nguyen, T. Q. Effect of Thermal Annealing on Polymer Light-Emitting Diodes Utilizing Cationic Conjugated Polyelectrolytes as Electron Injection Layers. *J. Phys. Chem. C* **2010**, *114*, 15786–157900.
- (43) Na, S.-I.; Oh, S.-H.; Kim, S.-S.; Kim, D.-Y. Efficient Organic Solar Cells with Polyfluorene Derivatives as a Cathode Interfacial Layer. *Org. Electron.* **2009**, *10*, 496–500.
- (44) Di Pietro, R.; Sirringhaus, H. High Resolution Optical Spectroscopy of Air-Induced Electrical Instabilities in n-type Polymer Semiconductors. *Adv. Mater.* **2012**, *24*, 3367–3372.
- (45) Di Pietro, R.; Fazzi, D.; Kehoe, T. B.; Sirringhaus, H. Spectroscopic Investigation of Oxygen- and Water-Induced Electron Trapping and Charge Transport Instabilities in n-Type Polymer Semiconductors. *J. Am. Chem. Soc.* **2012**, *134*, 14877–14889.
- (46) Wei, P.; Oh, J. H.; Dong, G.; Bao, Z. Use of a 1H-Benzimidazole Derivative as an n-Type Dopant and To Enable Air-Stable Solution-Processed n-Channel Organic Thin-Film Transistors. *J. Am. Chem. Soc.* **2010**, *132*, 8852–8853.
- (47) Oh, J. H.; Wei, P.; Bao, Z. Molecular n-type Doping for Air-Stable Electron Transport in Vacuum-Processed n-Channel Organic Transistors. *Appl. Phys. Lett.* **2010**, *97*, 243305.
- (48) Wei, P.; Menke, T.; Naab, B. D.; Leo, K.; Riede, M.; Bao, Z. 2-(2-Methoxyphenyl)-1,3-Dimethyl-1H-Benzimidazol-3-ium Iodide as a New Air-Stable n-Type Dopant for Vacuum-Processed Organic Semiconductor Thin Films. *J. Am. Chem. Soc.* **2012**, *134*, 3999–4002.
- (49) Li, C.-Z.; Chueh, C.-C.; Ding, F.; Yip, H.-L.; Liang, P.-W.; Li, W.; Jen, A. K.-Y. Doping of Fullerenes via Anion-Induced Electron Transfer and Its Implication for Surfactant Facilitated High Performance Polymer Solar Cells. *Adv. Mater.* **2013**, *25*, 4425–4430.
- (50) Lee, S.-H.; Oh, S.-H.; Ji, Y.; Kim, J.; Kang, R.; Khim, D.; Lee, S.; Yeo, J.-S.; Lu, N.; Kim, M. J.; Ko, H. C.; Kim, T.-W.; Noh, Y.-Y.; Kim, D.-Y. Side Chains Contributions to Characteristics of Resistive Memory Based on Water-Soluble Polyfluorenes: Effects of Structure and Length of Side Pendant Group. *Org. Electron.* **2014**, *15*, 1290–1298.